Pharmacogenomics and Personalized Medicine

Dovepress

open access to scientific and medical research

Open Access Full Text Article

ORIGINAL RESEARCH

# Exploring the Correlation Between *GPR176*, a Potential Target Gene of Gastric Cancer, and Immune Cell Infiltration

Xianhua Gu[1,*], Honghong Shen[2,*], Zheng Xiang[3], Xinwei Li[2], Yue Zhang[2], Rong Zhang[1], Fang Su[2], Zishu Wang[2]

[1]Department of Gynecology Oncology, First Affiliated Hospital of Bengbu Medical College, Bengbu, People's Republic of China; [2]Department of Medical Oncology, First Affiliated Hospital of Bengbu Medical College, Bengbu, People's Republic of China; [3]Department of Surgical Oncology, First Affiliated Hospital of Bengbu Medical College, Bengbu, People's Republic of China

*These authors contributed equally to this work

Correspondence: Fang Su; Zishu Wang, Department of Medical Oncology, The First Affiliated Hospital of Bengbu Medical College, Anhui Province Key Laboratory of Translational Cancer Research, Bengbu Medical College, 287 Changhuai Road, Bengbu, Anhui, 233004, People's Republic of China, Tel +8613605523272; +86 18909620171, Email sufang2899@163.com; wzshahbb@163.com

**Introduction:** *GPR176*, an orphan G protein-coupled receptor (GPCR), is essential for the progression of gastrointestinal cancers. However, it is still unclear how *GPR176* affects tumor immunity and patient prognosis in gastric cancer (GC).

**Methods:** The Cancer Genome Atlas (TCGA) and Gene Expression Omnibus (GEO) were searched in this investigation to assess the expression patterns of *GPR176* in GC tissues and normal gastric mucosa. The findings were further verified using immunohistochemical tests and quantitative Real-Time Polymerase Chain Reaction (qRT-PCR). The Kaplan-Meier method, univariate logistic regression, and Cox regression were then used to investigate the relationship between *GPR176* and clinical traits. Additionally, the potential correlation between *GPR176*, immune checkpoint genes, and immune cell infiltration levels was investigated.

**Results:** As per the research findings, GC tissues had higher levels of *GPR176* than normal tissues. Additionally, individuals with high expression of *GPR176* had a worse 10-year overall survival (OS), in contrast with those having a low expression of *GPR176* ($p < 0.001$). The OS of GC can be predicted using a validated nomogram model. The expression of *GPR176* demonstrated a negative correlation with CD8+ T cells. When compared to the low-expression group of *GPR176*, Tumor Immune Dysfunction and Exclusion (TIDE) analysis demonstrated that the high-expression group had a considerably higher risk of immune evasion. A remarkable difference (variation) was observed in the levels of *GPR176* expression across both groups, ie, low and high-risk groups, as determined by the immune phenomenon scores (IPS) immunotherapy assessment.

**Conclusion:** By examining *GPR176* from various biological perspectives, it was determined that *GPR176* can act as a predictive biomarker for poor patient prognosis in GC. Additionally, it was observed that *GPR176* is capable of suppressing the proliferation of CD8+ T cells and facilitating immune evasion.

**Keywords:** *GPR176*, gastric cancer, tumor microenvironment, immunotherapy, immune escape

## Introduction

G protein-coupled receptors (GPCRs) have emerged as important pharmacological targets due to their numerous therapeutic uses.[1] These cell surface receptors represent the largest family of receptors and are involved in signaling various stimuli, such as hormones, growth factors, lipids, both peptide and non-peptide neurotransmitters, as well as light and smell.[2] *GPR176* belongs to a family of orphan GPCRs known for transcriptional responses in human breast cancer.[3,4] In vivo, *GPR176* undergoes N-glycosylation, a crucial modification that ensures the accurate expression and functionality of the protein.[5]

Received: 28 March 2023
Accepted: 26 May 2023
Published: 1 June 2023

GC occupies the fifth position in the worldwide prevalence of malignant cancers and constitutes the fourth leading cause of cancer-related deaths. The year 2020 witnessed almost 769,000 deaths attributed to GC.[6] The treatment modalities for GC include chemotherapy, radiation therapy, gastrectomy, targeted therapy, and immunotherapies.[7] Despite the recent advancements in therapeutic interventions, the mortality rate associated with GC remains substantially high.[8]

The tumor immune microenvironment (TIME) stimulates the progression of GC and is involved in patient prognosis.[9,10] TIME primarily consists of immune cells, tumor stem cells, fibroblasts, and extracellular matrix. The presence of tumor-infiltrating lymphocytes (TILs) and immune cells within the TIME can be used for predicting the prognosis of various malignancies.[11,12] In addition, TILs serve as reliable indicators of immunotherapeutic response.[11–13] Immune checkpoint inhibitors (ICI) have yielded modest survival benefits in GC, with anti-PD-1 therapy especially improving OS at 12 and 18 months, and have shown encouraging results in the treatment of a number of malignancies, including melanoma, Hodgkin's lymphoma, and glioma.[14–16] Thus, TIME is an important predictor of immune checkpoint blockade (ICB) response and improves the efficacy of current ICB therapy.

The purpose of the current investigation was to investigate the function of *GPR176* expression in the GC cohort and its association with prognosis. The association between *GPR176* expression, infiltrating immune cells, and markers of immune status were also explored. The findings suggested that *GPR176* possesses a significant role in immunotherapy and immune escape in GC.

# Methodology

## Dataset Source and Pre-Processing

33 TCGA pan-cancer data containing RNA sequencing (RNA-seq) expression profile data were downloaded from the UCSC Xena data portal (https://xenabrowser.net/). RNA sequencing (RNA-seq) data in the form of FPKM values for patients with GC, along with clinical data (including survival information) for 375 GC and 32 normal tissue samples, somatic mutation data, immune subtypes, methylation data, and clinical disease-specific survival (DSS), disease-free interval (DFI), and progression-free interval (PFI) data for pan-cancer patients were provided by the UCSC Xena and TCGA.[17–19] Additionally, the GEO dataset, comprising GSE13911, GSE66229, and GSE54129 as study subjects, was integrated (Table 1).[20] The R software (version 4.1.2) was employed to examine the expression levels of *GPR176* in GC and healthy gastric tissues.[21]

## Clinical Sample Collection

Samples were obtained from individuals who underwent GC surgery at the Department of Gastrointestinal Surgery of The First Affiliated Hospital of Bengbu Medical College between January 2017 and December 2018. Specifically, ten samples of GC tissue and their corresponding paraneoplastic tissues were obtained for qRT-PCR. In addition, 124 samples of GC tissue and 10 normal paraneoplastic tissues were collected for immunohistochemical staining. Notably, no patient received biological therapy, chemotherapy, or radiotherapy prior to or following surgery. The tissue samples were then kept at −80°C until protein extraction.

**Table 1** The Information of the Utilized GEO Datasets in Our Study

| Data set | Topics | Number of Samples |
|---|---|---|
| GSE13911 | Expression data from primary gastric tumors (MSI and MSS) and adjacent normal samples | 38 gastric tumors 31 normal gastric |
| GSE66229 | Molecular analysis of gastric cancer identifies discrete subtypes associated with distinct clinical characteristics and survival outcomes: the ACRG (Asian Cancer Research Group) study | 302 gastric tumor 98 normal gastric |
| GSE54129 | Global gene expression analysis of gastric cancer by oligonucleotide microarrays | 21 gastric tumors 111 normal gastric |

**Abbreviations**: GC, gastric cancer; GPR176, G protein-coupled receptor 176; TCGA, The Cancer Genome Atlas; GEO, Gene Expression Omnibus; OS, overall survival; GSEA, Gene set enrichment analysis; IHC, Immunohistochemistry; RT, room temperature; qRT-PCR, Quantitative reverse transcription polymerase chain reaction; DCs, resting dendritic cells; KM, Kaplan-Meier; FDR, false discovery rate; TME, tumor microenvironment; ICI, Immune checkpoint inhibitor; ICB, immune checkpoint blockade; MSigDB, Molecular Signatures Database; FDRs, false discovery rates; TIMER, Tumour Immune Estimation Resource; TCIA, The Cancer Immunome Database; IPS, immune phenomenon scores; TIDE, Tumour Immune Dysfunction and Exclusion.

## Experimental Materials

Abcam (ab122605) provided the rabbit anti-human antibody *GPR176* (100μL), UK. Moreover, Horseradish peroxidase (HRP) coupled with an anti-rabbit antibody was supplied by Jackson ImmunoResearch Inc. (US). Sigma-Aldrich provided bovine serum albumin (US). Sangon Biotech Co., Ltd. provided skimmed milk and Tween-20 (China). The TRIzol reagent was acquired from Thermo Fisher Scientific (US). TaKaRa (Japan) provided PrimeScriptTM 1st Strand cDNA Synthesis Kit, while TOYOBO (Japan) provided the SYBR Green Real-Time PCR Master Mix.

## Immunohistochemistry (IHC)

The tissue samples were fixed in 4% paraformaldehyde, paraffin-embedded, and sectioned before being attached to slides. These slides were subjected to deparaffinization, rehydration, and xylene density gradients. Antigen extraction was then accomplished using citrate buffer (pH 7.8, 0.1M) for 24 minutes at approximately 82°C. The endogenous peroxidase-blocking solution was uniformly applied to coat the slides for fifteen minutes at room temperature in order to prevent peroxidase activity. Overnight incubation with anti-*GPR176* primary antibody was carried out on the slides, followed by gentle rinsing with PBS. The slides were then exposed to a biotin-conjugated secondary antibody for 10 minutes at room temperature, followed by 5 minutes of incubation with streptavidin peroxidase. A hematoxylin dye wash was then used to remove any remaining debris from each slide. Hematoxylin dye wash was used to eliminate any residual debris on each slide. An immunohistochemistry examination could then be performed following slide drying and washing.

## Quantitative Real-Time Polymerase Chain Reaction (qRT-PCR)

To extract total RNA, TRIzol reagent was employed, followed by reverse transcription of the extracted RNA to produce DNA employing the RevertAid First Strand cDNA Synthesis Kit. SYBR Green Realtime PCR Master Mix was utilized to extract the cDNA. The primers utilized for qRT-PCR tests for human GRP176 were as follows: 5′-AAGGTGTTCTGCTCGGTGAC′ (forward) and 5′-GAGGGTAGAGGACTGAATAGTACCTG-3′ (reverse). GAPDH: 5′-AAGGTGTTCTGCTCGGTGAC-3′ (forward) and 5′-GAGGGTAGAGGACTGAATAGTACCTG-3′ (reverse) served as an internal control. Each sample from the respective groups was tested thrice, and the data from qRT-PCR were examined using paired Student's t-tests.

## Somatic Mutation Analysis

Two mutation profile groups (*GPR176*-high and *GPR176*-low) were developed through the comparative analysis of *GPR176* gene transcriptional levels in the initial cohort. The "oncoplot" function[22] in the "maftools" package[23] of the "R" was employed to create the mutation maps for the two groups. Subsequently, the "mafCompare" function[23] was used to evaluate the mutant gene distribution, which exhibited significant differences between the two groups.

## The Link of *GPR176* Expression with the Clinical Features of Individuals with GC

The median value of the *GPR176* expression was utilized to determine the expression threshold. To examine the association between *GPR176* expression and the clinical characteristics of patients with GC, univariate logistic regression was used. The Kaplan-Meier curve and the Log rank test were used to compare the 10-year OS.

## Constructing and Evaluating the Nomogram for Individuals with GC

To predict the OS of patients with GC at 1, 3, and 5 years, a nomogram model was developed based on the results of the univariate and multivariate Cox regression analyses. The "RMS" package[24] of the 'R' was utilized for the assessment of the nomogram. Calibration curves were constructed to compare the actual values with the predicted probabilities by the nomogram, using the Kaplan-Meier method. A well-calibrated nomogram prediction model revealed scatter points that fall on a 45° diagonal line. The Harrell concordance index (C-index), which ranged from 0.5 to 1, was used to evaluate the accuracy of the predictions made by the nomogram model. There was a 0.05 significance level for each test in all two-tailed statistical analyses in the present research.

## Evaluation of the Immunological Features of the Tumor Microenvironment (TME) of GC

To examine the relationship between *GPR176* expression and immune cell infiltration, the immune infiltration levels of 22 immune cell types were estimated by the "preprocessCore" package[25] and CIBERSORT algorithm.[26] In addition, the link between the expression of *GPR176* and 22 immune checkpoint molecules was assessed using the TCGA database and Tumour Immune Estimation Resource (TIMER).[27] P-value <0.05 indicated the significant level.

## Functional Analyses of *GPR176* in GC

To gain insight into the roles played by *GPR176* in GC, Gene Ontology (GO) and Kyoto Encyclopedia of Genes and Genomes (KEGG) functional enrichment analyses were done by clusterProfiler package. The three categories of the GO enrichment analysis were biological processes, cellular components, and molecular functions. Moreover, enrichment analyses of DEGs (DEGs) were carried out using the clusterProfiler tool, and a bubble graph was created to show the key signaling pathways linked to these DEGs. The candidate genes were divided into two groups for gene set enrichment analysis (GSEA) based on the mean of the risk score: high-risk group and low-risk group. The Molecular Signatures Database, MSigDB (https://www.gsea-msigdb.org/gsea/msigdb), provided functional predefined gene sets. The candidate genes involved in the pathway with the screening criteria of $p < 0.05$ and false discovery rate (FDR) < 0.25 were considered significantly enriched. The normalized enrichment score and adjusted p-value were used to identify signaling pathways that are significantly enriched.

## Statistical Analysis

The data analysis in this research was conducted utilizing R software (version 4.1.2),[28] GSEA (version 4.2.3),[29] and Perl (version 5.32.1.1).[30] The statistical methodologies employed in the investigation were described, along with the relevant R software packages employed. A cut-off criterion of $p < 0.05$ was established.

# Results

## The Level of *GPR176* Expression Was Elevated in Human Gastric Tissues

The differential expression analysis of Pan-cancer revealed varying expression levels of *GPR176* across different types of cancers. Notably, *GPR176* was significantly downregulated in invasive breast carcinoma, kidney chromophobe, and other types of cancers, while it was significantly upregulated in GC, cholangiocarcinoma, and other cancers ($p < 0.05$, Figure 1A). The expression of *GPR176* was further validated using information from TCGA and GEO datasets GSE13911, GSE66229, and GSE54129. The statistical significance criterion for all datasets was $p < 0.001$ (Figure 1B–E). Additionally, evaluation of the expression levels of *GPR176* mRNA in 32 pairs of adjacent normal and tumor tissues from the TCGA database revealed that the expression level was considerably greater in the tumor tissues than in adjacent healthy tissues ($p < 0.001$, Figure 1F). Moreover, qRT-PCR analysis showed that GC tissues expressed more *GPR176* mRNA than normal tissues ($p < 0.01$, Figure 1G). Immunohistochemical staining of GC tissues and paraneoplastic tissues showed that *GPR176* levels were considerably elevated in GC tissues in contrast with those in paraneoplastic tissues (Figure 1H). We retrieved the Immunohistochemical staining data from the Human Protein Atlas (HPA).[31] Immunohistochemical staining also showed that *GPR176* levels were higher in GC tissues than in paraneoplastic tissues (Supplementary Figure S1A–D).

## Prognostic Analysis of *GPR176* in GC

In order to determine the prognostic value of GPR176 in GC, the Kaplan-Meier method was used to verify the survival of GC patients with varying levels of GPR176 expression in TCGA and two online databases. The results showed that low-GPR176 expression individuals had a better 10-year OS as compared to those with high expression ($p < 0.05$, Figure 2A–C). The expression data of GPR176 and survival information from the TCGA database were combined, and we then plotted ROC curves for 1-, 3-, and 5-year patient survival, where the area under the curve (AUC) was 0.586 for 1 year, 0.649 for 3 years, and 0.793 for 5 years. These findings indicated that the ROC curve for GPR176 expression was relatively less accurate in predicting the 1-year and 3-year survival but more accurate in predicting 5-year survival with relatively high accuracy

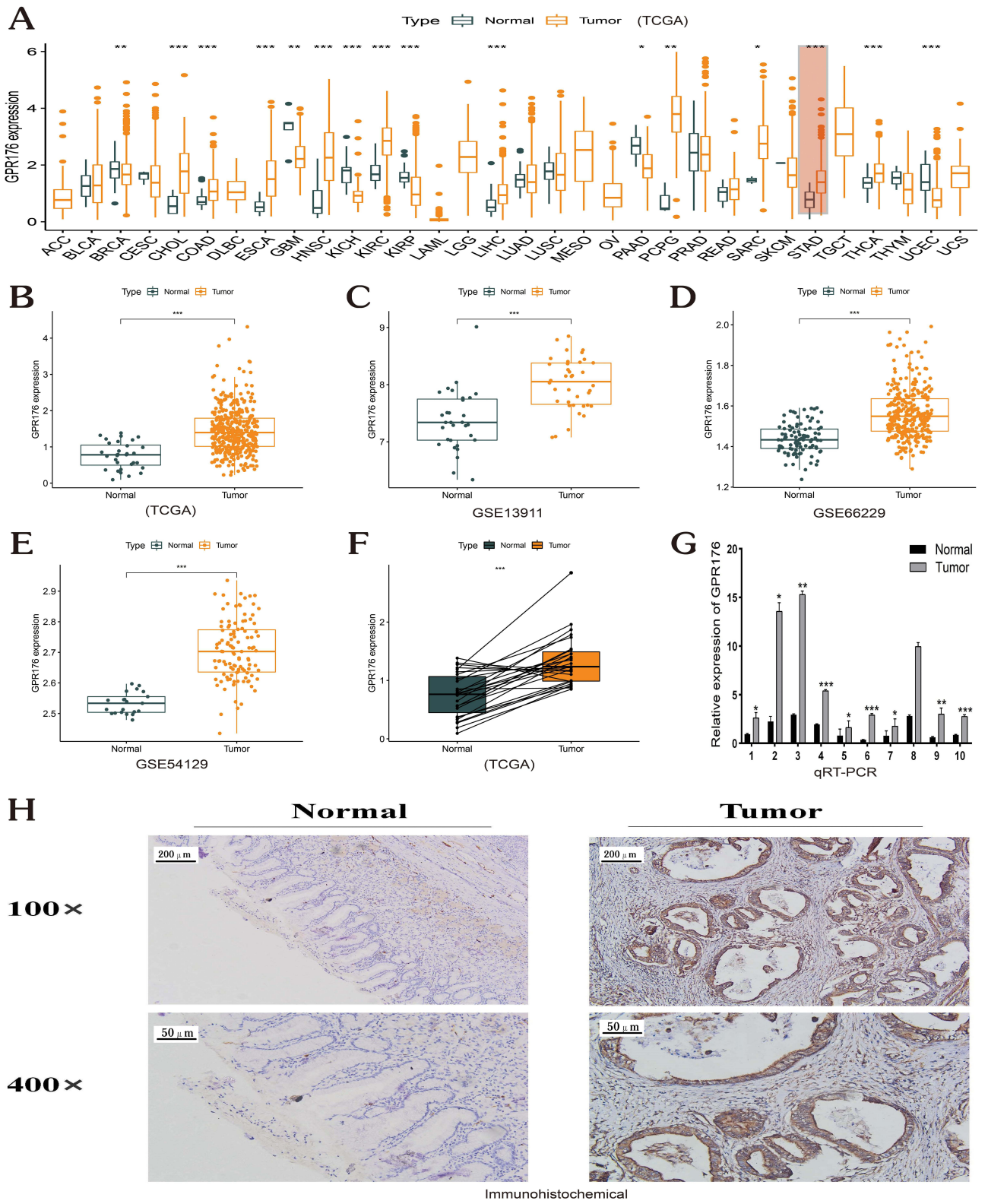


**Figure 1** *GPR176* expression in cancer tissues and surrounding normal tissues. (**A**) Variation in *GPR176* expression between tumor and healthy tissues in pan-cancer. (**B**) Upregulation of *GPR176* expression in the TCGA cohort. The GSE13911 (**C**), GSE66229 (**D**), and GSE54129 (**E**) datasets exhibit an increase in *GPR176* expression in GC tissue. (**F**) *GPR176* overexpression in the tumor as compared to the paraneoplastic tissues in the TCGA cohort. (**G**) A remarkable increase in *GPR176* expression in GC tissues as compared to healthy tissues using qRT-PCR. (**H**) An analysis of immunohistochemical staining indicating higher expression of *GPR176* in GC as compared to adjoining healthy tissues. The p-values for significance levels are denoted by *p < 0.05; **p < 0.01; ***p < 0.001.

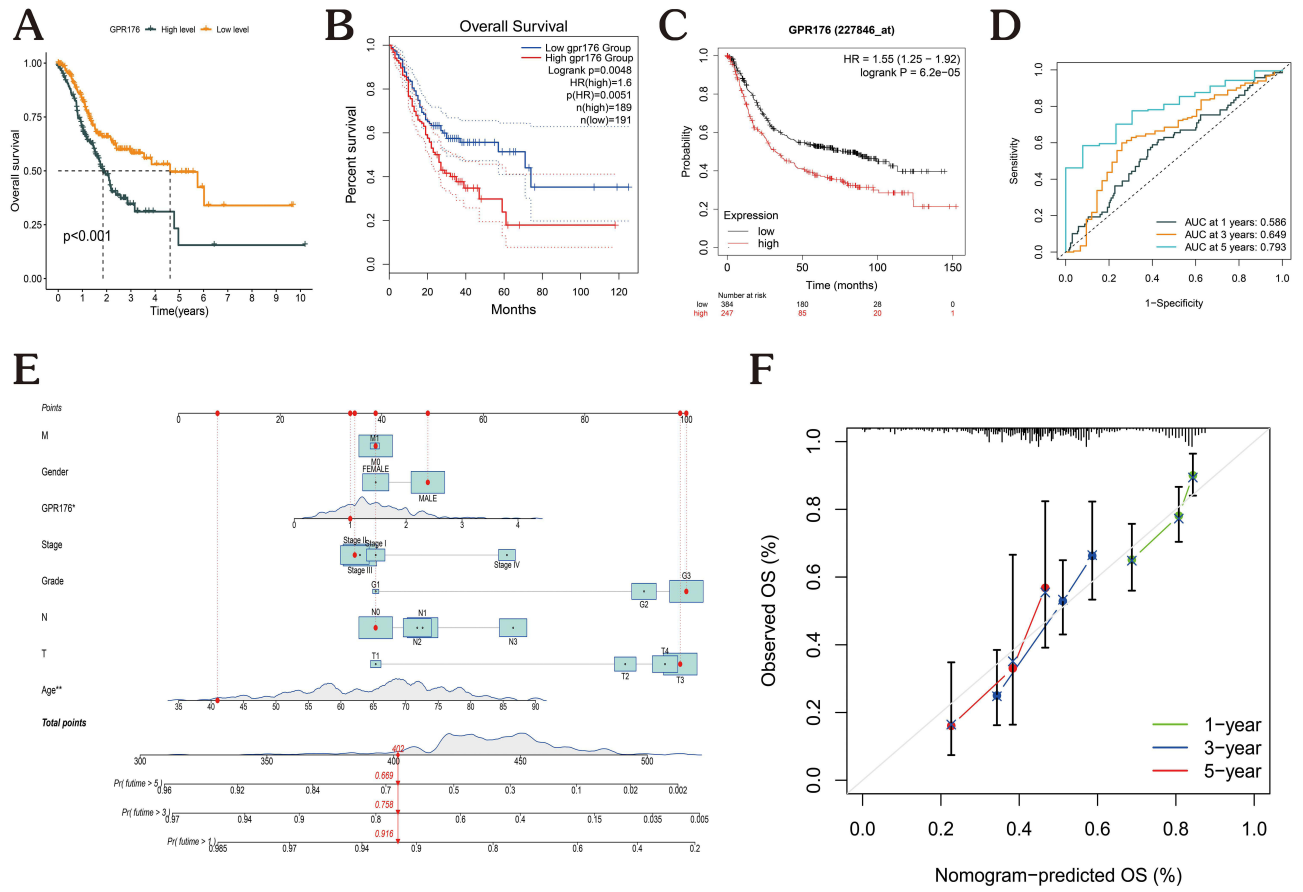


**Figure 2** Prognostic analysis of *GPR176* in GC. (**A**) The Kaplan-Meier analysis of OS of individuals with GC based on the *GPR176* gene expression in the TCGA database. (**B** and **C**) The association of *GPR176* expression with OS in GC patients using the Kaplan-Meier Plotter and GEPIA online databases, respectively. (**D**) The Receiver Operating Characteristic (ROC) curves of *GPR176* expression. (**E**) A nomogram model that was established to predict the 1-, 3-, and 5-year OS probability of individuals with GC. (**F**) The calibration curves of the nomogram model for predicting the probability of the 1-, 3-, and 5-year OS of individuals with GC. (*p < 0.05; **p <0.01).

(Figure 2D). A nomogram was created in an attempt to provide a novel model for predicting the prognosis in individuals with GC (Figure 2E). It was discovered that the bias-corrected 1, 3, and 5-year lines of the calibration plot were relatively close to the ideal 45° diagonal line, demonstrating that the theoretical and observed values were in accordance (Figure 2F). The above-mentioned results revealed that the nomogram model can be used to predict OS of individuals with GC. We also found that high GPR176 expression was an unfavorable predictor of GC DSS (p = 0.039), and it could not be used as a predictor of PFI (p = 0.148) and DFI (P=0.474) (Figure 3A–C). Univariate Cox regression analysis showed that pathological stage and age were strongly associated with the OS of GC patients and that GPR176 had a statistically significant prognostic value for GC patients (p = 0.006, Figure 3D). Further multivariate analysis showed that pathological stage and age were strongly associated with the OS of GC patients and that the prognostic value of GPR176 for GC patients was not statistically significant (p = 0.068, Figure 3E). Together, our results suggest that upregulated GPR176 expression predicts a poorer prognosis for GC patients.

## Link of *GPR176* Expression Level with Clinicopathological Features and Prognostic Significance of Individuals with GC

After eliminating any duplicates from the dataset, the investigation included 375 patients, of which 241 (64.3%) were males, and 134 (35.7%) were females. The findings indicate that *GPR176* expression levels were correlated with T-phase, stage, and G-phase (Figure 4A–G). Additionally, a correlation heat map was constructed (Figure 4H), revealing that the *GPR176* gene is most likely involved in tumor progression.

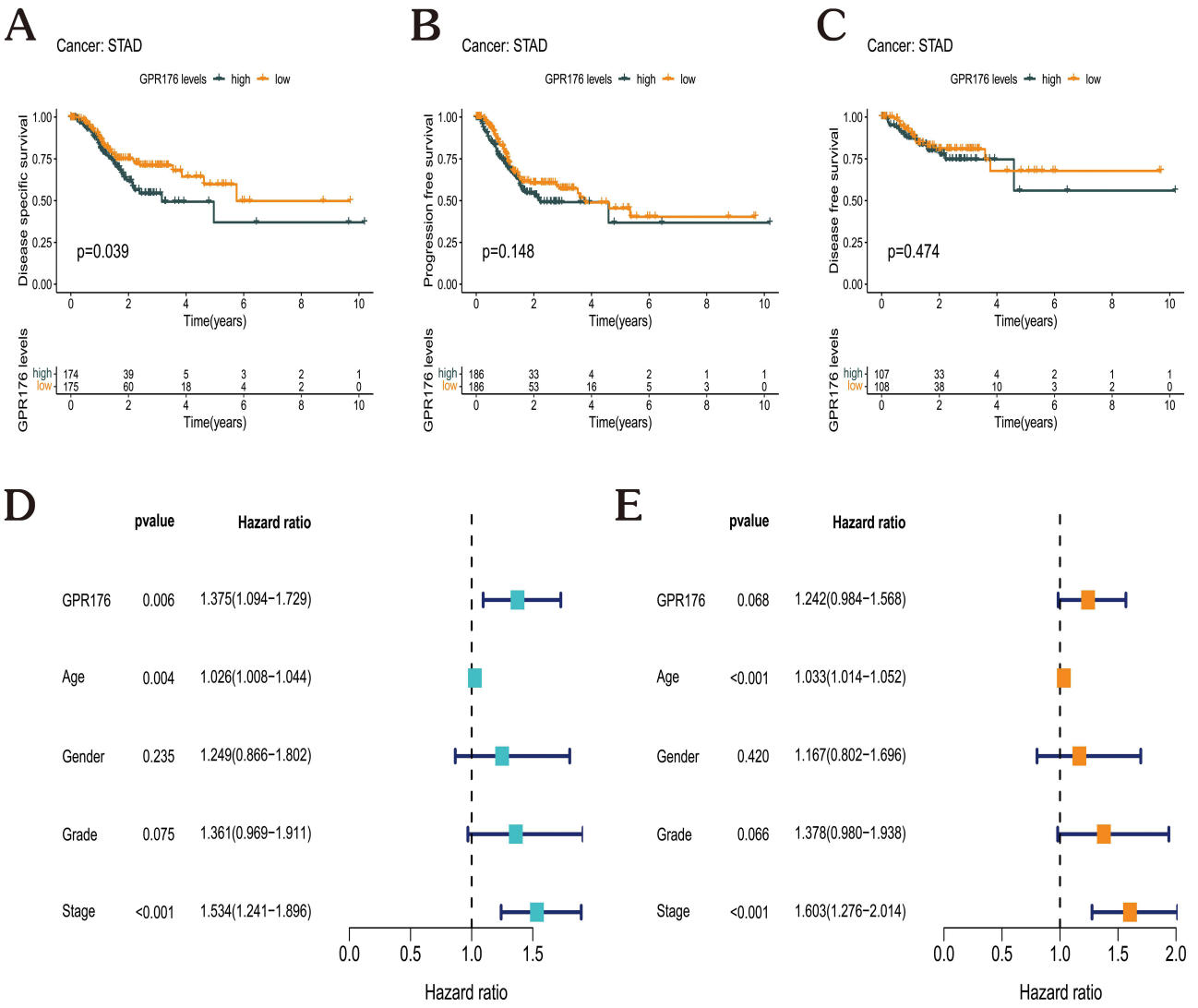


**Figure 3** Prognostic analysis of *GPR176* in GC. (**A**–**C**) Kaplan-Meier analysis of DSS, PFS and DFS of GC patients with *GPR176* gene expression in the TCGA database. (**D** and **E**) The results of univariate (**D**) and multivariate Cox regression (**E**) for the OS of patients with GC are shown in forest plots.

## Expression of *GPR176* in GC in Relation to Somatic Mutations, Methylation, Tumor Mutational Load, and TME

The 20 genes exhibiting the highest mutation frequencies were separately plotted for the low- and high-expression groups. The findings suggest that genes with low expression exhibited higher mutation frequencies. For instance, TTN had a lower mutation rate in the high-*GPR176* cohort when compared to the low-*GPR176* cohort (40% vs 53%, Figure 5A and B). Gene co-expression circle plots were generated using GC expression in the TCGA database, revealing that *GPR176* showed a positive correlation with *MMP2, KIRREL, PDGFRB, ANTXR1, NID2*, and *FSTL1*, as well as a negative correlation with *TSN, ATP5MK, CXO4I1, COX7B*, and *ATP5MC3* (Figure 5C). The mean methylation value of all methylation sites in the *GPR176* gene was used to obtain the methylation degree of the gene, revealing a negative relationship between the *GPR176* expression and its methylation degree ($R = -0.13$, $p = 0.017$, Figure 5D). Furthermore, *GPR176* expression presented a negative correlation with the tumor mutational burden (TMB) ($R = -0.26$, $p < 0.001$, Figure 5E). TME scores were then calculated for the low- as well as high-expression groups of *GPR176*, using GC expression profiles in the TCGA database and the "estimate" package[32] in R language. Subsequent TME differential analysis indicated upregulation of the ImmuneScore, ESTIMATEScore, and StromalScore of TMB in the high expression group of *GPR176* (Figure 5F).

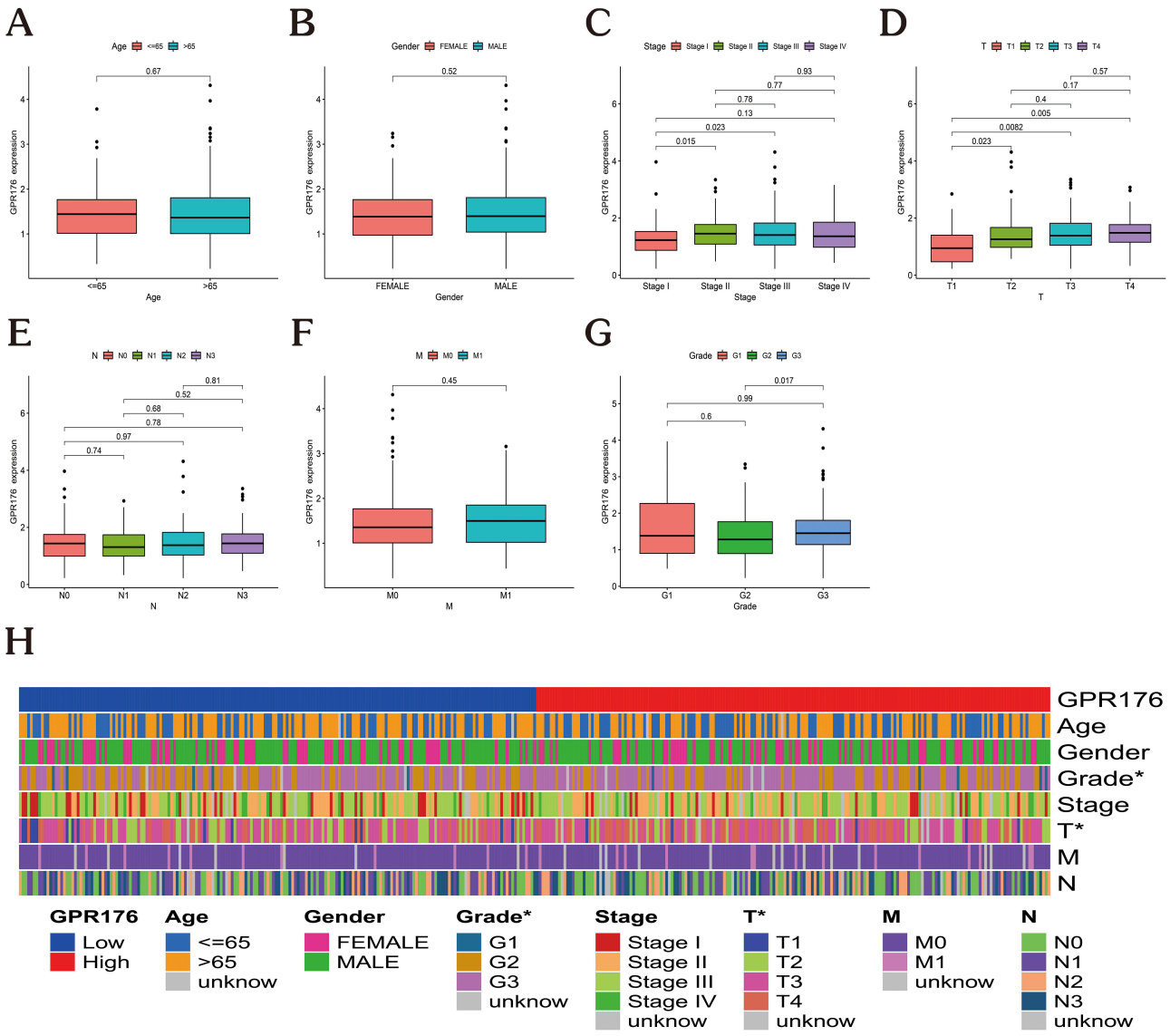


**Figure 4** Link of *GPR176* expression level with clinicopathological features. (**A**–**G**) The link between *GPR176* expression level and various clinicopathological features for age (**A**), gender (**B**), stage (**C**), T classification (**D**), N classification (**E**), M classification (**F**), and Grade (**G**). (**H**) A heatmap showing the relationship between *GPR176* expression level and the clinicopathological features of individuals with GC. (*p < 0.05).

## Functional Analysis of *GPR176* in GC

The samples from GC were classified into low- and high-*GPR176* expression groups. The DEGs between the two groups were identified using fdrFilter = 0.05, and 1061 DEGs were identified. A heat map was generated to visualize the DEGs (Figure 6A). To further explore the role of the discovered genes, KEGG and GO analyses were performed. The KEGG analysis showed that DEGs were considerably enriched in the pathways related to calcium signaling, PI3K-Akt signaling, and neuroactive ligand-receptor interaction (Figure 6B and C). The GO analysis of biological processes revealed that these DEGs were involved in the formation and organization of the extracellular matrix as well as the organization of extracellular structures. The cellular component analysis also revealed that DEGs were enriched in the extracellular matrix that contains collagen, and the neuronal cell body. A molecular function analysis revealed that DEGs were primarily found in the extracellular matrix structural component and glycosaminoglycan binding (Figure 6D–F).

GSEA analysis was utilized to show the ten leading pertinent signaling pathways of *GPR176* in GC (Figure 6G). The enrichment analysis results showed that pathways associated with cellular functional structure and differentiation as well as immune and inflammatory responses were enriched in the *GPR176* high expression group, including focal adhesion,

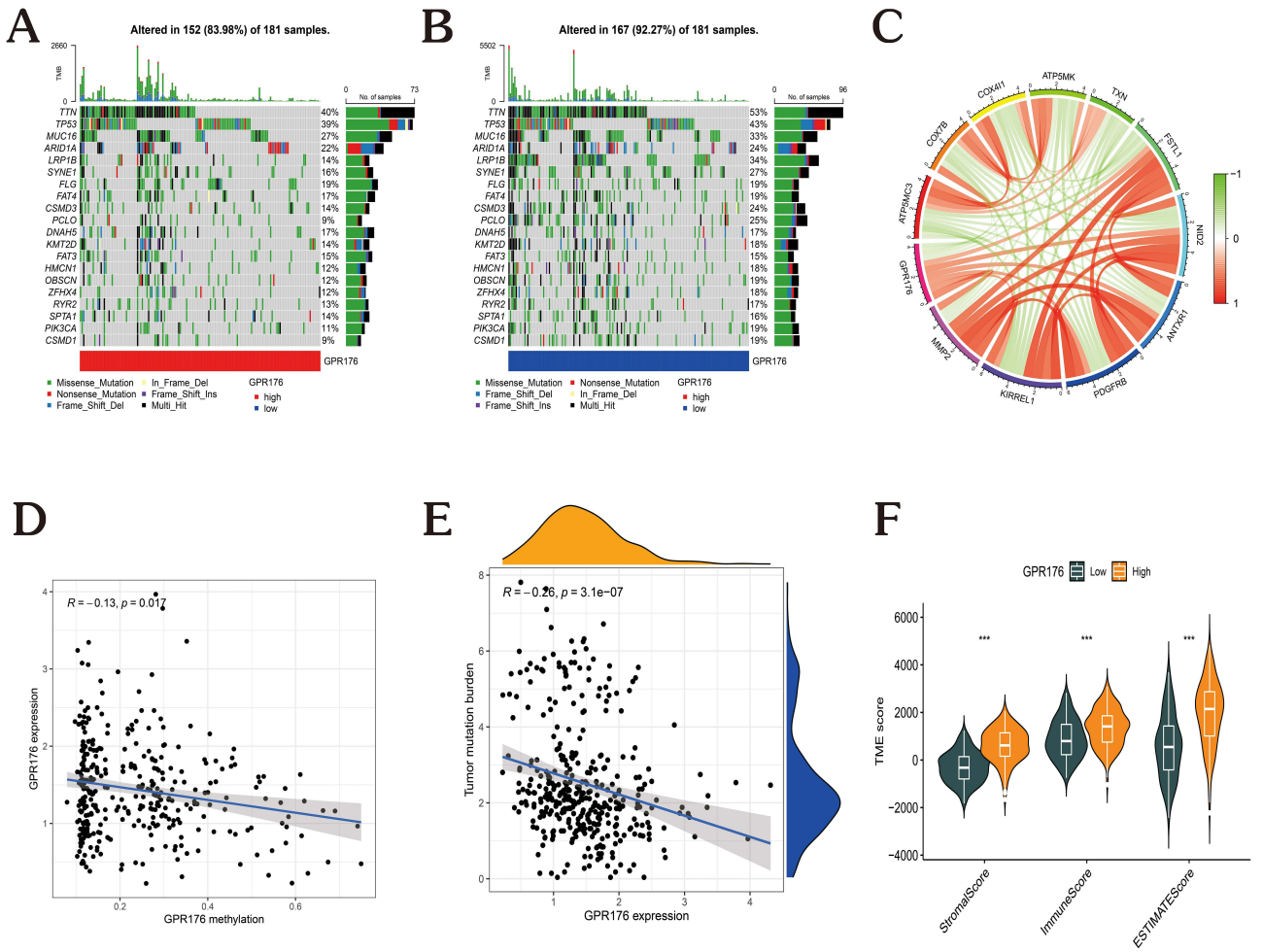


**Figure 5** Expression of *GPR176* in GC in relation to somatic mutations, methylation, TMB, and TME. (**A** and **B**) Somatic mutations in high- and low-*GPR176* expression groups. (**C**) *GPR176* co-expression analysis. The red connecting line highlights a positive correlation, and the green line highlights a negative correlation. (**D**) Correlation analysis of *GPR176* gene's expression and methylation. (**E**) Correlation analysis of the *GPR176* gene's expression with the TMB. (**F**) StromalScore, ImmuneScore, and ESTIMATEScore of the TME differed between the high and low *GPR176* expression groups. (***p < 0.001).

ECM receptor interaction, chemokine signaling pathway, cell adhesion molecules cams (Figure 6H–K). Collectively, these findings indicate that *GPR176* is an immune-linked gene that might be involved in the inflammatory response, angiogenesis, and tumor immune response, promoting gastric carcinogenesis and progression.

## Correlation Analysis of GRP176 Expression with 22 GC Common Immune Checkpoint Genes

Next, the interaction of GPR176 with 22 immune checkpoint genes was analyzed (Figure 7). The findings highlighted that 15 of the 22 immune checkpoint genes were remarkably higher in the high-GPR176 expression group than in the low-expression group (Figure 7A, P<0.05). Using the Tumor Immune Estimation Resource (TIMER) site[33] we also found that the expression levels of most immunological checkpoint molecules, such as CD274, CTLA4, and PDCD1, were positively linked with GPR176 expression levels (Figure 7B–W, P<0.05). Therefore, it could be hypothesized that GPR176 may be involved in the regulation of immune cell infiltration patterns.

## *GPR176* Inhibits the Proliferation of CD8+ T Cells and Mediates Immune Escape in GC

The study utilized the CIBERSORT algorithm to validate the association between *GPR176* and immune cells. To categorize patients with C based on *GPR176* expression, the median expression was used to create low- and high-

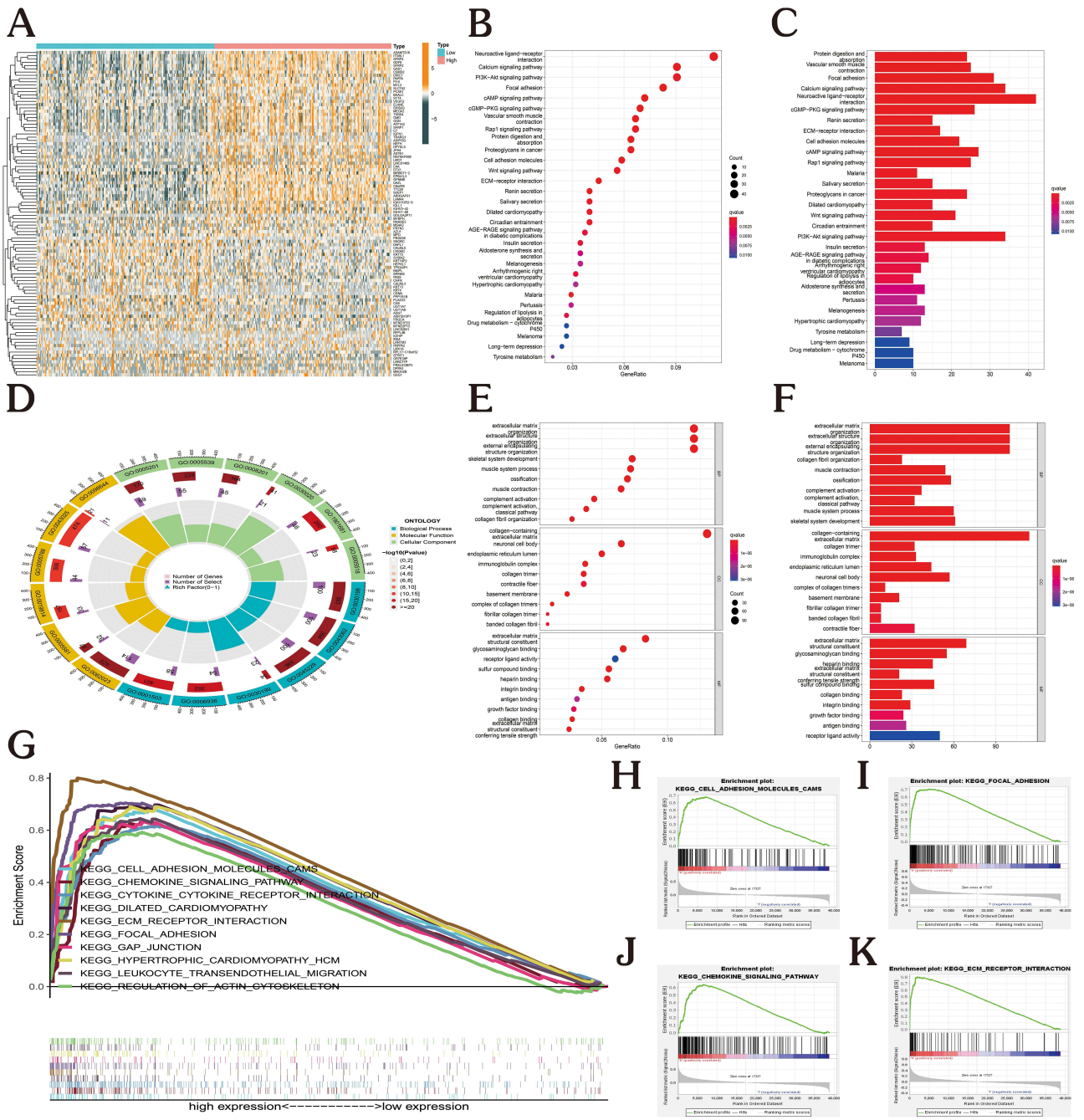


**Figure 6** Functional analysis of *GPR176* in GC. (**A**) Heatmap of differential genes in *GPR176*-high and *GPR176*-low expression groups. (**B** and **C**) KEGG enrichment analysis of *GPR176*. (**D–F**) GO function annotation of *GPR176*. (**G-K**) *GPR176* gene set enrichment analysis.

expression groups. The proportion of 22 immune cell types was compared in the two groups (Figure 8A). *GPR176* was negatively associated with T cells CD8, resting mast cells, activated NK cells, and macrophages M1 and positively associated with macrophages M0, activated mast cells, and macrophages M2 (Figure 8B–I, P<0.05). Analysis performed using TIMER[33] revealed that *GPR176* expression in XCELL[34] and EPICS[35] algorithms was negatively correlated with CD8+ T cells (Figure 8K and L). Prior studies have classified the TME into two subtypes, an inflammatory TME dominated by T-cell infiltration and a non-inflammatory TME dominated by T-cell suppression. Tumors with T-cell inflammation contain abundant CD8+ T cells and CD8α/CD103-lineage DCs, while tumors without T-cell inflammation lack these cells but contain blood vessels, macrophages, and fibroblasts, thus supporting tumor growth.[36,37] This study

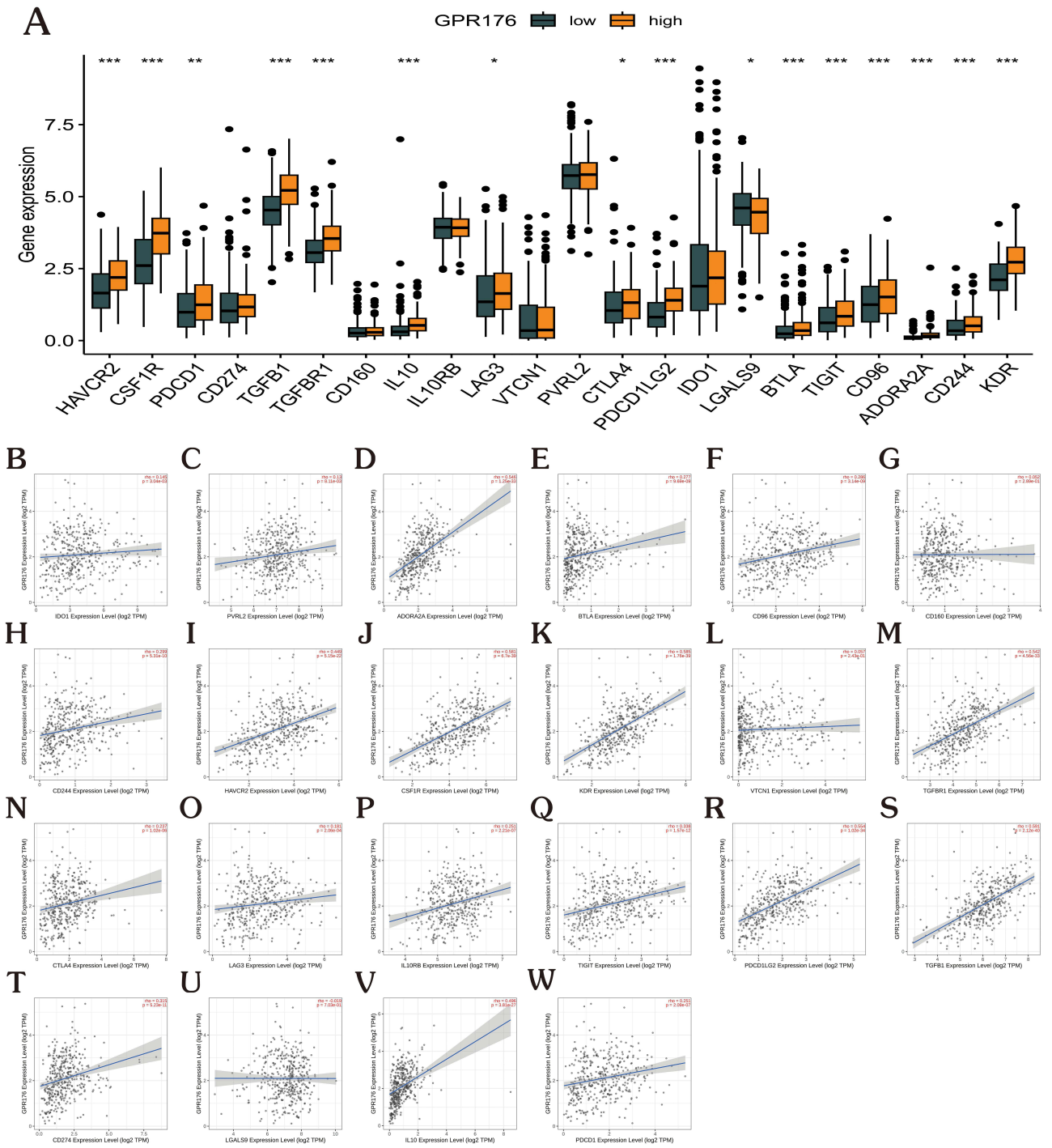


**Figure 7** Correlation analysis of GRP176 expression with 22 GC common immune checkpoint genes. (**A**) Differential expression of 22 immune checkpoint genes between high and low *GPR176* groups in GC (*p < 0.05; **p <0.01; ***p < 0.001). (**B**–**W**) Correlation of GPR176 in GC with 22 immune checkpoint genes in the TIMER portal (P<0.05).

proposes that *GPR176* shapes a non-inflammatory TME (immune-exclusion phenotype) in GC. Also, the Tumor Immune Dysfunction and Exclusion (TIDE)[38] scores were considerably greater in the group with high *GPR176* expression compared to the group with low *GPR176* expression, showing that high *GPR176* expression contributes to immune evasion in the GC-related tumor immune microenvironment (TIME) (Figure 8J).

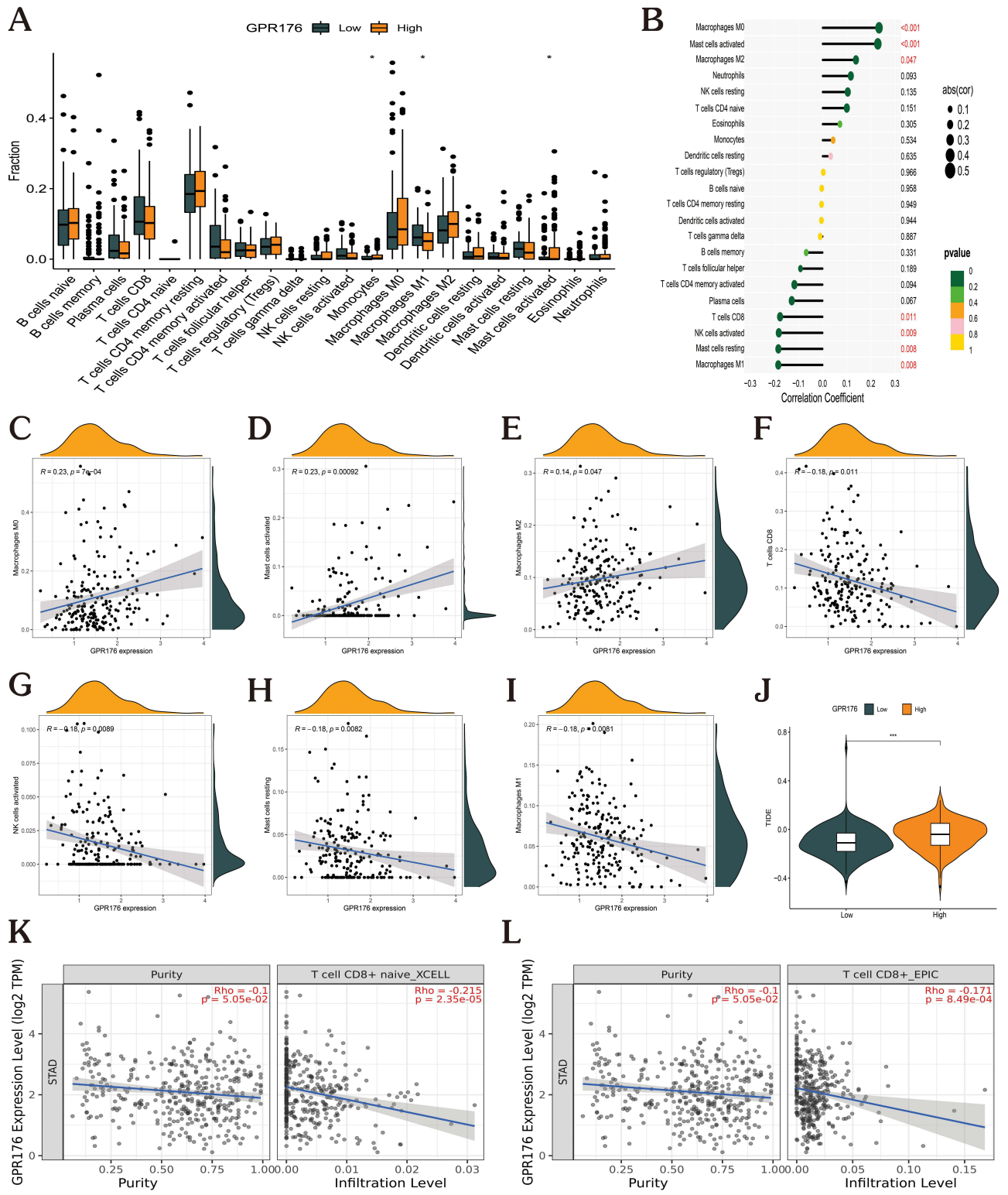


**Figure 8** *GPR176* inhibits the proliferation of CD8+ T cells and mediates immune escape in GC. (**A**) Box plots based on *GPR176* expression analysis differences with 22 immune cell types in GC. (**B**) Correlation between *GPR176* expression and 22 immune cell types in GC. (**C**–**E**) *GPR176* expression was positively linked to macrophages M0, activated mast cells, and macrophages M2. (**F**–**I**) *GPR176* expression was negatively correlated with T cells CD8, NK cells activated, Mast cells resting, and Macrophages M1. (**J**) Assessment of immune evasion efficacy in the high- and low-*GPR176*-expression groups. (**K**–**L**) *GPR176* expression in XCELL33 and EPICS34 algorithms was negatively correlated with CD8+ T cells. (*p < 0.05; ***p < 0.001).

## Expression of *GPR176* in GC and Evaluation of Clinical Treatment

The R language "pRRophetic" package was utilized to produce box plots illustrating the drug treatment sensitivity in patients belonging to high- and low-*GPR176* expression groups (pFilter = 0.001). A total of 63 drugs associated with *GPR176* treatment were selected (Figure 9A–D, Supplementary Figures S2 and S3. Patients with GC exhibiting high *GPR176* expression levels demonstrated sensitivity to ciprofloxacin and dasatinib treatments while displaying insensitivity to 5-fluorouracil and bosutinib. Analysis of immune phenomenon scores (IPS) through TCIA,[39] revealed remarkable variation in the efficacy of various immunotherapies between the low and high *GPR176* expression groups (Figure 9E–H).

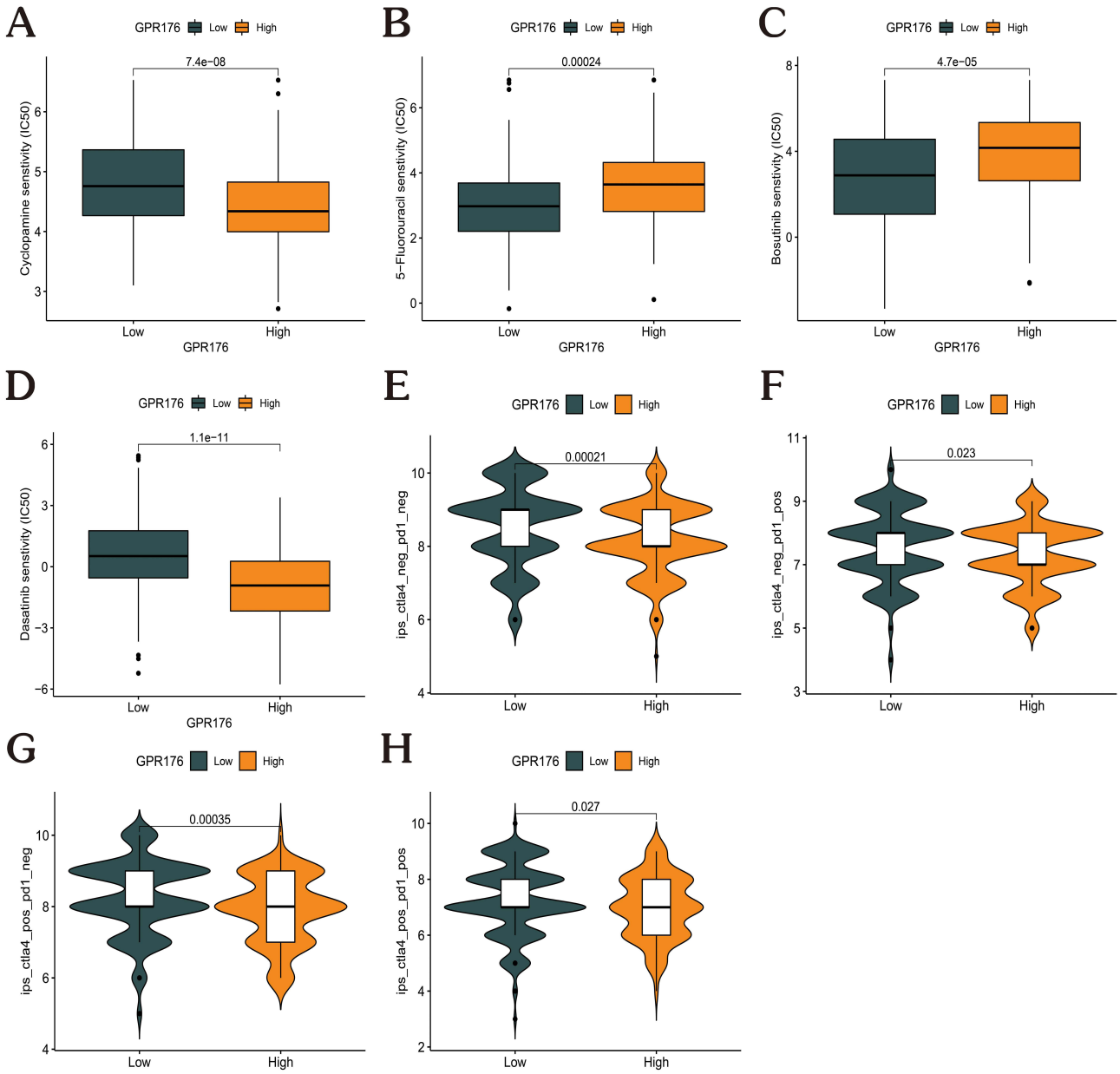


**Figure 9** Expression of *GPR176* in GC and evaluation of clinical treatment. (**A**–**D**) Differences in drug treatment sensitivity of Ciprofloxacin (**A**), 5-fluorouracil (**B**), Bosutinib (**C**), and Dasatinib (**D**) between the high and low *GPR176* groups. (**E**–**H**) The link of IPS with the *GPR176* expression in individuals with GC based on the TCIA database; CTLA4- PD1- (**E**), CTLA4- PD1+ (**F**), CTLA4+ PD1- (**G**), CTLA4+PD1+ (**H**).


https://doi.org/10.2147/PGPM.S411199 DovePress

## Discussion

To date, no prior research had been performed on the relationship between *GPR176* and GC. In this study, it was revealed that GC tissues had significantly higher levels of *GPR176* expression. The survival analysis found a link between high *GPR176* expression and a poor prognosis in GC. ROC analysis suggests that *GPR176* may serve as a predictive biomarker with a low predictive value (AUC between 0.7–0.8 was considered moderate). Furthermore, high *GPR176* expression is considerably linked to the grade and T stage of the GC. Therefore, *GPR176* may function as a biomarker for a poor prognosis in GC.

There is substantial proof to validate the vital role of GPCRs in the progression of gastrointestinal cancers.[40] One orphan GPCR, *GPR176*, which is rich in SCN, has been implicated in the regulation of the biological clock in the suprachiasmatic nucleus as well as in the transcriptional response of human breast cancer.[3,41] GPCRs are a known class of cell surface molecules that performs a very important role in signaling and have recently been implicated in the development and metastasis of tumors.[42] Many GPCRs are linked to tumor formation, progression, invasion, and metastasis. In addition, GPCRs contribute to establishing and maintaining a microenvironment that allows tumor formation and growth, including effects on the peripheral vasculature, signaling molecules, and extracellular matrix.[43] GPCRs are targeted by about 30% of currently available medications, making them the most common group of gene products.[44] Mutations in GPCRs can lead to acquired and inherited diseases, including retinitis pigmentosa, hypothyroidism, hyperthyroidism, nephrogenic uremia, fertility disorders, and cancer.[45]

Previous research has clearly shown a link between immune escape, tumor immune infiltration, and cancer prognosis and treatment responsiveness.[46–48] The majority of the tumor cells produce antigens that can mediate recognition by host CD8+ T cells. Immune escape can be separated into two groups based on the TMB. One major subset displays a T cell-inflamed phenotype and resists immune attack through the dominant inhibitory effects of immune system-suppressive pathways. The other subset lacks this phenotype and resists an immune attack by either excluding or ignoring the immune system.[49] For a molecule to be an effective target for cancer immunotherapy, it must demonstrate TME-specific overexpression and immunosuppressive function.[50] To identify the prospective role of *GPR176* in GC and its expression in the TME, GC cohorts were analyzed from 3 GEO datasets of the TCGA database. The findings revealed that *GPR176* expression was considerably overexpressed in GC tumor tissues, which was confirmed by qRT-PCR and immunohistochemical experiments. The current study also revealed that *GPR176* was negatively associated with the immunological status of TME in GC, and *GPR176* positively correlated with most immune checkpoints in GC, including *LAG-3, PD-L1, PD-1*, and *CTLA-4*, that suppress the effector function of T cells and impede the anti-tumor immunity of the body. Using the CIBERSORT algorithm, a remarkable downregulation was observed in the activity of T cell recruitment in the high *GPR176* group, *GPR176* was correlated negatively with CD8+ T cell and NK cell activation, and the level of TIIC infiltration was significantly reduced. These findings highlight that *GPR176* could inhibit the proliferation of CD8+ T cells so as promote immune escape. Subsequently, the TIDE score revealed a greater potential for immune escape in the high *GPR176* group. Therefore, targeting *GPR176* in GC could reduce the potential for immune escape and thus enhance the efficacy of immunotherapy. Our study has some limitations. Our exploration of the role of *GPR176* in GC was based on data from the GEO and TCGA databases. However, we did not perform relevant experiments to confirm the link between *GPR176* and immune cells infiltrating TME, which points the way for our future work. Secondly, the effect of *GPR176* with patient immunotherapy was obtained through TCGA database analysis, which currently lacks direct evidence, and this will be the focus of our future work. In addition, the relationship between *GPR176* expression in GC and somatic mutation, methylation, tumor mutational load and tumor microenvironment as well as the functional analysis of *GPR176* in GC need to be further explored, and this part can complement single cell level studies and provide insight into the mechanism of *GPR176* in gastric cancer, which will also be the focus of our future studies and experiments.

## Conclusion

According to this research, the *GPR176* expression level is considerably higher in GC tissues than in healthy tissues. This suggests that *GPR176* could be used as a novel biomarker to distinguish between GC tissues and healthy gastric mucosa. Upregulated *GPR176* was linked strongly to poor OS, progression-free interval, and disease-specific survival in GC

patients. Further development and computational validation of a nomogram model for individualized OS assessment were performed. Functional annotation and pathway enrichment analysis supported that *GPR176* is primarily involved in the inflammatory response, angiogenesis, and tumor immune response. Immune cell infiltration analysis revealed that *GPR176* inhibited the proliferation of CD8+ T cells and promoted immune escape. The comprehensive assessment of *GPR176* as a potential prognostic biomarker for GC also broadens the horizons in immunotherapy and may offer a reliable evaluation system for clinical use.

## Data Sharing Statement

This study analysed used clinical data publicly available in the following online databases: TCGA (https://www.cancer.gov/), GEO (https://www.ncbi.nlm.nih.gov/geo/), GEPIA (http://gepia2.cancer-pku.cn/), Kaplan-Meier Plotter (Kaplan-Meier plotter [Gastric] (kmplot.com)), TIMER (TIMER2.0 (comp-genomics.org)), TCIA (https://tcia.at/), TIDE (http://tide.dfci.harvard.edu/).

## Ethics Approval and Informed Consent

The Ethics Committee of the First Affiliated Hospital of Bengbu Medical College [2022] 372 has examined and granted its approval for the research involving human subjects. The study was conducted in adherence to the Helsinki Declaration, which lays out ethical principles for medical research involving human subjects. Patients/participants gave their consent to be involved in this research through the signing of a consent form. Informed consent was provided by all patients.

## Acknowledgments

We express our gratitude to Bullet Edits Limited for their valuable contributions to language editing and proofreading of the manuscript. We also acknowledge the open databases, including TCGA, GEO, GEPIA, TIMER, TCIA and TIDE, for providing the necessary platform and datasets for this research.

## Author Contributions

All authors made a significant contribution to the work reported, whether that is in the conception, study design, execution, acquisition of data, analysis and interpretation, or in all these areas; took part in drafting, revising or critically reviewing the article; gave final approval of the version to be published; have agreed on the journal to which the article has been submitted; and agree to be accountable for all aspects of the work.

## Funding

The present study was supported by the College Student Innovation Training Program of Bengbu Medical College (grant no. Byycx 22110), 512 Talent Cultivation Plan of Bengbu Medical College (grant numbers by51201319), Research and Innovation Team of Bengbu Medical College (grant no. BYKC201908). University Scientific research project of Education Department of Anhui Province (grant no. KJ2021A0714). Provincial education and Teaching research project (grant no. 2021jyxm0954).

## Disclosure

The authors report no conflicts of interest in this work.

## References

1. Nakagawa S, Nguyen Pham KT, Shao X, Doi M. Time-restricted g-protein signaling pathways via GPR176, Gz, and RGS16 set the pace of the master circadian clock in the suprachiasmatic nucleus. *Int J Mol Sci*. 2020;21(14):5055. doi:10.3390/ijms21145055
2. Yang D, Zhou Q, Labroska V, et al. G protein-coupled receptors: structure- and function-based drug discovery. *Signal Transduct Target Ther*. 2021;6(1):7. doi:10.1038/s41392-020-00435-w
3. Wang T, Nakagawa S, Miyake T, et al. Identification and functional characterisation of N-linked glycosylation of the orphan G protein-coupled receptor Gpr176. *Sci Rep*. 2020;10(1):4429. doi:10.1038/s41598-020-61370-y

4. Schultz DJ, Krishna A, Vittitow SL, et al. Transcriptomic response of breast cancer cells to anacardic acid. *Sci Rep*. 2018;8(1):8063. doi:10.1038/s41598-018-26429-x
5. Doi M, Murai I, Kunisue S, et al. Gpr176 is a Gz-linked orphan G-protein-coupled receptor that sets the pace of circadian behaviour. *Nat Commun*. 2016;7(1):10583. doi:10.1038/ncomms10583
6. Sung H, Ferlay J, Siegel RL, et al. Global cancer statistics 2020: GLOBOCAN estimates of incidence and mortality worldwide for 36 cancers in 185 countries. *CA Cancer J Clin*. 2021;71(3):209–249. doi:10.3322/caac.21660
7. Xie J, Fu L, Jin L. Immunotherapy of gastric cancer: past, future perspective and challenges. *Pathol Res Pract*. 2021;218:153322. doi:10.1016/j.prp.2020.153322
8. Alkasalias T, Moyano-Galceran L, Arsenian-Henriksson M, Lehti K. Fibroblasts in the tumor microenvironment: shield or spear? *Int J Mol Sci*. 2018;19(5):1532. doi:10.3390/ijms19051532
9. Li W, Zhang X, Wu F, et al. Gastric cancer-derived mesenchymal stromal cells trigger M2 macrophage polarization that promotes metastasis and EMT in gastric cancer. *Cell Death Dis*. 2019;10(12):918. doi:10.1038/s41419-019-2131-y
10. Wang H, Wu X, Chen Y. Stromal-immune score-based gene signature: a prognosis stratification tool in gastric cancer. *Front Oncol*. 2019;9:1212. doi:10.3389/fonc.2019.01212
11. Mantovani A, Romero P, Palucka AK, Marincola FM. Tumour immunity: effector response to tumour and role of the microenvironment. *Lancet*. 2008;371(9614):771–783. doi:10.1016/S0140-6736(08)60241-X
12. Fridman WH, Pages F, Sautes-Fridman C, Galon J. The immune contexture in human tumours: impact on clinical outcome. *Nat Rev Cancer*. 2012;12(4):298–306. doi:10.1038/nrc3245
13. Liu F, Yang Z, Zheng L, et al. A tumor progression related 7-gene signature indicates prognosis and tumor immune characteristics of gastric cancer. *Front Oncol*. 2021;11:690129. doi:10.3389/fonc.2021.690129
14. Zappasodi R, Merghoub T, Wolchok JD. Emerging concepts for immune checkpoint blockade-based combination therapies. *Cancer Cell*. 2018;33(4):581–598. doi:10.1016/j.ccell.2018.03.005
15. Khasraw M, Reardon DA, Weller M, Sampson JH. PD-1 inhibitors: do they have a future in the treatment of glioblastoma? *Clin Cancer Res*. 2020;26(20):5287–5296. doi:10.1158/1078-0432.CCR-20-1135
16. Kono K, Nakajima S, Mimura K. Current status of immune checkpoint inhibitors for gastric cancer. *Gastric Cancer*. 2020;23(4):565–578. doi:10.1007/s10120-020-01090-4
17. Tomczak K, Czerwinska P, Wiznerowicz M. The Cancer Genome Atlas (TCGA): an immeasurable source of knowledge. *Contemp Oncol*. 2015;19(1A):A68–A77.
18. Blum A, Wang P, Zenklusen JC. SnapShot: TCGA-analyzed tumors. *Cell*. 2018;173(2):530. doi:10.1016/j.cell.2018.03.059
19. Goldman MJ, Craft B, Hastie M, et al. Visualizing and interpreting cancer genomics data via the xena platform. *Nat Biotechnol*. 2020;38(6):675–678. doi:10.1038/s41587-020-0546-8
20. Clough E, Barrett T. The gene expression omnibus database. *Methods Mol Biol*. 2016;1418:93–110.
21. Chan BKC. Data Analysis Using R Programming. *Adv Exp Med Biol*. 2018;1082:47–122.
22. Li Y, Bian Y, Wang K, Wan XP. POLE mutations improve the prognosis of endometrial cancer via regulating cellular metabolism through AMF/AMFR signal transduction. *BMC Med Genet*. 2019;20(1):202. doi:10.1186/s12881-019-0936-2
23. Mayakonda A, Lin DC, Assenov Y, Plass C, Koeffler HP. Maftools: efficient and comprehensive analysis of somatic variants in cancer. *Genome Res*. 2018;28(11):1747–1756. doi:10.1101/gr.239244.118
24. Liu TT, Li R, Huo C, et al. Identification of CDK2-related immune forecast model and ceRNA in lung adenocarcinoma, a pan-cancer analysis. *Front Cell Dev Biol*. 2021;9:682002. doi:10.3389/fcell.2021.682002
25. Mehdi T, Bailey SD, Guilhamon P, Lupien M, Kelso J. C3D: a tool to predict 3D genomic interactions between cis-regulatory elements. *Bioinformatics*. 2019;35(5):877–879. doi:10.1093/bioinformatics/bty717
26. Chen B, Khodadoust MS, Liu CL, Newman AM, Alizadeh AA. Profiling tumor infiltrating immune cells with CIBERSORT. *Methods Mol Biol*. 2018;1711:243–259.
27. Li T, Fu J, Zeng Z, et al. TIMER2.0 for analysis of tumor-infiltrating immune cells. *Nucleic Acids Res*. 2020;48(W1):W509–W514. doi:10.1093/nar/gkaa407
28. Giorgi FM, Ceraolo C, Mercatelli D. The R language: an engine for bioinformatics and data science. *Life*. 2022;12(5):648. doi:10.3390/life12050648
29. Powers RK, Goodspeed A, Pielke-Lombardo H, Tan AC, Costello JC. GSEA-InContext: identifying novel and common patterns in expression experiments. *Bioinformatics*. 2018;34(13):i555–i564. doi:10.1093/bioinformatics/bty271
30. Suwazono S, Arao H. A newly developed free software tool set for averaging electroencephalogram implemented in the Perl programming language. *Heliyon*. 2020;6(11):e05580. doi:10.1016/j.heliyon.2020.e05580
31. Digre A, Lindskog C. The human protein atlas-spatial localization of the human proteome in health and disease. *Protein Sci*. 2021;30(1):218–233. doi:10.1002/pro.3987
32. Wu J, Li L, Zhang H, et al. A risk model developed based on tumor microenvironment predicts overall survival and associates with tumor immunity of patients with lung adenocarcinoma. *Oncogene*. 2021;40(26):4413–4424. doi:10.1038/s41388-021-01853-y
33. Li T, Fan J, Wang B, et al. TIMER: a web server for comprehensive analysis of tumor-infiltrating immune cells. *Cancer Res*. 2017;77(21):e108–e110. doi:10.1158/0008-5472.CAN-17-0307
34. Aran D, Hu Z, Butte AJ. xCell: digitally portraying the tissue cellular heterogeneity landscape. *Genome Biol*. 2017;18(1):220. doi:10.1186/s13059-017-1349-1
35. Zheng H, Liu H, Ge Y, Wang X. Integrated single-cell and bulk RNA sequencing analysis identifies a cancer associated fibroblast-related signature for predicting prognosis and therapeutic responses in colorectal cancer. *Cancer Cell Int*. 2021;21(1):552. doi:10.1186/s12935-021-02252-9
36. Gajewski TF, Corrales L, Williams J, Horton B, Sivan A, Spranger S. Cancer immunotherapy targets based on understanding the T cell-inflamed versus non-T cell-inflamed tumor microenvironment. *Adv Exp Med Biol*. 2017;1036:19–31.
37. Garris CS, Luke JJ. Dendritic cells, the T-cell-inflamed tumor microenvironment, and immunotherapy treatment response. *Clin Cancer Res*. 2020;26(15):3901–3907. doi:10.1158/1078-0432.CCR-19-1321

38. Fu J, Li K, Zhang W, et al. Large-scale public data reuse to model immunotherapy response and resistance. *Genome Med*. 2020;12(1):21. doi:10.1186/s13073-020-0721-z
39. Prior FW, Clark K, Commean P, et al. TCIA: an information resource to enable open science. *Annu Int Conf IEEE Eng Med Biol Soc*. 2013;2013:1282–1285. doi:10.1109/EMBC.2013.6609742
40. Zeng Z, Ma C, Chen K, et al. Roles of G Protein-Coupled Receptors (GPCRs) in gastrointestinal cancers: focus on sphingosine 1-shosphate receptors, angiotensin ii receptors, and estrogen-related GPCRs. *Cells*. 2021;10(11). doi:10.3390/cells10112988
41. Goto K, Doi M, Wang T, Kunisue S, Murai I, Okamura H. G-protein-coupled receptor signaling through Gpr176, Gz, and RGS16 tunes time in the center of the circadian clock [Review]. *Endocr J*. 2017;64(6):571–579. doi:10.1507/endocrj.EJ17-0130
42. Dorsam RT, Gutkind JS. G-protein-coupled receptors and cancer. *Nat Rev Cancer*. 2007;7(2):79–94. doi:10.1038/nrc2069
43. Liu Y, An S, Ward R, et al. G protein-coupled receptors as promising cancer targets. *Cancer Lett*. 2016;376(2):226–239. doi:10.1016/j.canlet.2016.03.031
44. Ribeiro-Oliveira R, Vojtek M, Goncalves-Monteiro S, et al. Nuclear G-protein-coupled receptors as putative novel pharmacological targets. *Drug Discov Today*. 2019;24(11):2192–2201. doi:10.1016/j.drudis.2019.09.003
45. Schoneberg T, Schulz A, Biebermann H, Hermsdorf T, Rompler H, Sangkuhl K. Mutant G-protein-coupled receptors as a cause of human diseases. *Pharmacol Ther*. 2004;104(3):173–206. doi:10.1016/j.pharmthera.2004.08.008
46. Lawal B, Lin LC, Lee JC, et al. Multi-omics data analysis of gene expressions and alterations, cancer-associated fibroblast and immune infiltrations, reveals the onco-immune prognostic relevance of STAT3/CDK2/4/6 in human malignancies. *Cancers*. 2021;13(5):954. doi:10.3390/cancers13050954
47. Vinay DS, Ryan EP, Pawelec G, et al. Immune evasion in cancer: mechanistic basis and therapeutic strategies. *Semin Cancer Biol*. 2015;35(Suppl):S185–S198. doi:10.1016/j.semcancer.2015.03.004
48. Jhunjhunwala S, Hammer C, Delamarre L. Antigen presentation in cancer: insights into tumour immunogenicity and immune evasion. *Nat Rev Cancer*. 2021;21(5):298–312. doi:10.1038/s41568-021-00339-z
49. Kaderbhai C, Tharin Z, Ghiringhelli F. The role of molecular profiling to predict the response to immune checkpoint inhibitors in lung cancer. *Cancers*. 2019;11(2):201. doi:10.3390/cancers11020201
50. Sanmamed MF, Chen L. A paradigm shift in cancer immunotherapy: from enhancement to normalization. *Cell*. 2018;175(2):313–326. doi:10.1016/j.cell.2018.09.035